Ling et al. *NPG Asia Materials* (2023) 15:19
https://doi.org/10.1038/s41427-023-00461-4

NPG Asia Materials

ARTICLE Open Access

Ultrastrong and fatigue-resistant bioinspired conductive fibers via the in situ biosynthesis of bacterial cellulose

Zhang-Chi Ling[1], Huai-Bin Yang[1], Zi-Meng Han[1], Zhan Zhou[1], Kun-Peng Yang[1], Wen-Bin Sun[1], De-Han Li[1], Hao-Cheng Liu[1], Chong-Han Yin[1], Qing-Fang Guan[1] and Shu-Hong Yu[1,2]

Abstract

High-performance functional fibers play a critical role in various indispensable fields, including sensing, monitoring, and display. It is desirable yet challenging to develop conductive fibers with excellent mechanical properties for practical applications. Herein, inspired by the exquisite fascicle structure of skeletal muscle, we constructed a high-performance bacterial cellulose (BC)/carbon nanotube (CNT) conductive fiber through in situ biosynthesis and enhancement of structure and interaction. The biosynthesis strategy achieves the in situ entanglement of CNTs in the three-dimensional network of BC through the deposition of CNTs during the growth of BC. The structure enhancement through physical wet drawing and the interaction enhancement through chemical treatment facilitate orientation and bridging of components, respectively. Owing to the ingenious design, the obtained composite fibers integrate high strength (939 MPa), high stiffness (52.3 GPa), high fatigue resistance, and stable electrical performance, making them competitive for constructing fiber-based smart devices for practical applications.

Introduction

The modern world has never stopped innovating high-performance functional fibers, which have greatly promoted the development of sensing, energy conversion, biomedicine, and other fields[1–5]. In particular, conductive fibers feature the combination of mechanical flexibility and high conductivity and possess great potential for the functionalization and intellectualization of fiber-based composites and devices, making them one of the most important fiber materials[6–9]. However, commercially available conductive fibers are always based on metals and suffer from low fatigue resistance, resulting in limited mechanical performance in practical applications[10]. Therefore, many efforts have been made to improve the mechanical properties of conductive fibers for better application in various complex situations. Numerous studies have explored the coating and doping of conductive materials to stretchable polymers, which are widely employed in the construction of highly ductile and flexible conductive fibers[11–15]. Despite these recent advances, challenges remain as to how to construct conductive composite fibers with the combination of high strength and high fatigue resistance, which play a key role in technical fields, such as aerospace and automobiles[16,17].

Biomimetic design holds great promise to improve the strength and fatigue resistance of materials. By imitating the optimized natural structure, bioinspired materials can demonstrate improved performance that often surpasses that of their components[18–20]. Skeletal muscle, one of the most interesting models, has oriented muscle fascicles with muscle fibers embedded in an endomysium network through

Correspondence: Qing-Fang Guan (guanqf@ustc.edu.cn) or Shu-Hong Yu (shyu@ustc.edu.cn)
[1]Department of Chemistry, Institute of Biomimetic Materials & Chemistry, Anhui Engineering Laboratory of Biomimetic Materials, Division of Nanomaterials & Chemistry, Hefei National Research Center for Physical Sciences at the Microscale, University of Science and Technology of China, Hefei, China
[2]Institute of Innovative Materials, Department of Materials Science and Engineering, Department of Chemistry, USTC-SUSTech Joint Research Center for Advanced Materials, Southern University of Science and Technology, Shenzhen, China

bridging proteins (such as integrin and dystrophin), a structure which possesses obvious advantages in dispersing and transmitting stress, giving muscles stability and excellent mechanical properties[21–25]. Therefore, mimicking the structure of muscle fascicles by uniformly embedding one-dimensional nanomaterials in a three-dimensional (3D) network through appropriate interaction bridging between components, is expected to possess a similar effect, laying an effective pathway toward high-performance fiber materials.

Herein, inspired by the exquisite fascicle architecture of skeletal muscle resulting in excellent mechanical properties, we report a new method for fabricating an ultrastrong and fatigue-resistant bacterial cellulose (BC)/carbon nanotube (CNT) conductive fiber by in situ biosynthesis with enhancement in structure and interaction. During this preparation, an aerosol-assisted biosynthesis strategy is employed to achieve nanomaterial assembly in the growth of BC, uniformly entangling CNTs in situ in the 3D network of BC. After that, the wet-drawing and wet-twisting procedures contribute to the oriented and dense structure inside composite fibers, and chemical treatment for component bridging effectively enhances the interactions between the components. As a result of the physical and chemical enhancement, CNTs are tightly embedded in the oriented 3D network of BC, similar to the muscle fascicle structure of skeletal muscle. Owing to this exquisite bioinspired design, the composite fibers achieve high strength (939 MPa), high stiffness (52.3 GPa) and fatigue resistance while ensuring electrical conductivity through the connections of CNTs. Therefore, these muscle-inspired fibers exhibit stable performance in long-term service, indicating great potential to construct high-performance smart devices for practical applications.

Results and discussion

Material fabrication and characterization

BC, a high-strength crystalline cellulose with a 3D network structure formed by cellulose nanofibers, possesses great potential as a robust platform for the construction of functional composites through biosynthesis[26–28]. Based on such a platform, inspired by the exquisite fascicle structure of skeletal muscle, high-performance BC/CNT conductive fibers were constructed through in situ biosynthesis and enhancement in structure and interaction.

Inside the muscle fascicles of skeletal muscle, the endomysium network surrounds and links muscle fibers to form a tightly connected whole, which plays an important role in force transmission, thereby providing the muscle with excellent mechanical properties. Herein, the muscle-inspired composite structure of a BC network with CNTs was realized through an aerosol-assisted biosynthesis strategy. The first step is the inoculation of the bacterial strain, i.e., *Gluconacetobacter xylinus* 1.1812, on the solid agar substrate to form a thin pure BC film. After that, through the spray of filtered compressed air, the CNT solution was transformed into a uniform aerosol and fed onto the BC film. Therefore, CNTs are deposited in real time on the interface between BC and air during the secretion of BC, enabling in situ composite preparation (Fig. 1a). As a result, similar to the in situ entanglement of muscle fibers in the endomysium network, CNTs are uniformly entangled in situ by the 3D network of BC, forming a robust composite hydrogel (Fig. 1b). Notably, this biosynthetic composite hydrogel features a continuous 3D physical network, as the secretion of BC is a continuous process, giving it great potential in mechanical performance.

Due to the 3D network of BC, the strips cut from the composite hydrogel can withstand the large physical deformation caused by wet drawing, causing them to gradually dehydrate and transform into dense composite fibers (Fig. 1c). Through repeatedly wet drawing and shaking BC strips until they can no longer be stretched, an oriented structure was constructed with CNTs entangled in the 3D network of BC (Fig. 1g), which corresponds to the exquisite, oriented fascicle structure of muscle (Fig. 1f). Then, the repeated alternating wet twisting and shaft smoothing process further densified and shaped the BC strips into dense fibers. Finally, the composite fibers were successively chemically treated with 3-aminopropyltriethoxysilane (APTES) and 1-pyrenebutyrie acid *N*-hydroxysuccinimide ester (PSE), thereby introducing PSE to BC and forming BC-PSE (Fig. 1d, e and Fig. S1)[29–31]. Benefitting from the aromatic functional groups provided by PSE, π-π interactions can be formed between BC-PSE and CNTs (Fig. 1g), which is similar to the protein bridging inside muscle fascicles and effectively enhances the combination between the components (Fig. 1f). Through this exquisite muscle-inspired design with physical and chemical enhancement, dense muscle-inspired fibers are endowed with higher mechanical strength than most natural fibers (Fig. 1e, h and Table S1), making it promising to construct high-performance fiber-based composite materials and devices[32–37].

To verify the validity of this strategy, the morphologies and properties of the composite fibers were systematically characterized. Through the aerogel-assisted biosynthesis strategy, CNTs are uniformly distributed in the 3D network of BC (Fig. 2a and Figs. S2, S3), which is attributed to the in situ deposition of CNTs during the growth of BC. Benefiting from the 3D network structure of BC, the obtained composite hydrogel is endowed with excellent robustness, allowing it to withstand the structural changes caused by wet drawing. During the wet drawing process, the BC strips gradually shrink in the radial direction, expand in the axial direction, and finally realize the oriented structure and densification of the composite strips, which are confirmed by scanning electron microscopy (SEM) images (Fig. 2d, e, g and h).

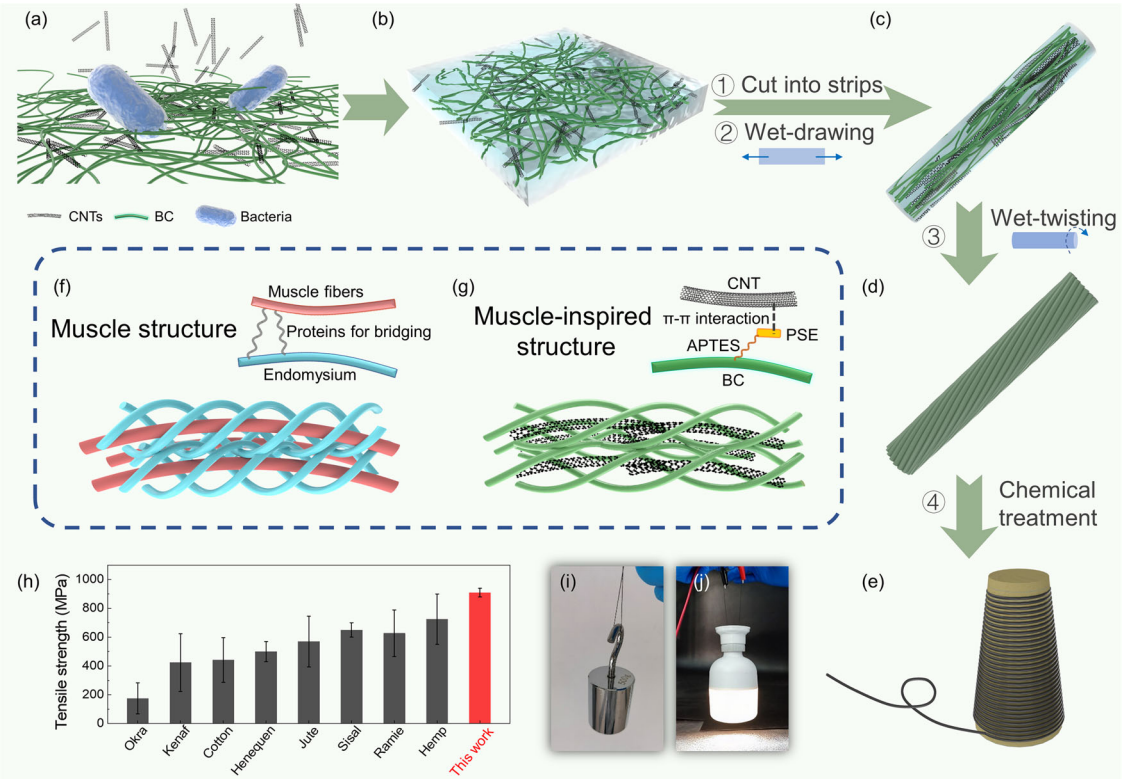

Fig. 1 Fabrication of the muscle-inspired fibers. a Schematic illustration of the in situ composite preparation through the in situ aerosol-assisted biosynthesis process. Carbon nanotubes (CNTs) are continuously settled and entangled by bacterial cellulose (BC) nanofibers. **b** The composite hydrogel with CNTs uniformly distributed in the 3D network of BC. **c** The obtained hydrogel strips are transformed into oriented fibers through wet drawing. **d** After wet twisting, the composite fibers are further densified and shaped. **e** After chemical treatment, muscle-inspired fibers are obtained. **f** The exquisite fascicle structure of skeletal muscle with muscle fibers embedded in the 3D network of the endomysium through proteins for bridging. **g** The muscle-inspired structure with CNTs embedded in the 3D network of BC through π–π interactions. **h** The tensile strength of the muscle-inspired fibers is higher than that of typical natural fibers. **i** The muscle-inspired fibers with a diameter of approximately 0.21 mm can stably be loaded with a weight of 0.5 kg. **j** The muscle-inspired fibers are used to hang a light bulb.

As shown in Fig. 2d, the obtained composite fibers with only wet twisting, named BC/CNT fibers, feature many undulating folds on the rough surface, which is due to substantial dehydration during the air-drying process of fibers[38]. At high magnification, this rough surface exhibits an isotropic microstructure composed of randomly oriented CNTs and BC nanofibers (Fig. 2e), demonstrating the inherent structure of biosynthetic samples in the absence of wet drawing. In contrast, the composite fibers with wet drawing and wet twisting, named WD-BC/CNT fibers, show smoother surfaces owing to the reduced water content and densification during the wet-drawing procedure (Fig. 2g). Meanwhile, highly aligned BC nanofibers with reduced pore sizes can be observed in the high-magnification SEM image of WD-BC/CNT fibers (Fig. 2h). Through 2D-WAXD measurement and analysis, the degree of orientation of WD-BC/CNT fibers reached 47% (Fig. 2i), which is significantly higher than that of BC/CNT fibers (9%) (Fig. 2f). Moreover, due to the uniform distribution of CNTs in the 3D network of BC, WD-BC/CNT fibers possess a higher degree of orientation than pure BC fibers (33%) under the same degree of wet drawing (~24%) (Fig. S4).

The oriented wet-drawing and wet-twisting processes contribute to the alignment and densification of composite fibers, yet the lack of interaction between CNTs and BC nanofibers hinders the binding of the internal components. To overcome this obstacle, the WD-BC/CNT fibers were first silanized with APTES to introduce amino groups, and then PSE reacted with the amino groups to form BC-PSE, thereby achieving the components bridging through π-π interactions between BC-PSE and CNTs (Fig. 1g and Figs. S1, S5)[29,30]. As shown in Fig. 2c, the obtained fibers, named muscle-inspired fibers, fluoresce under ultraviolet light, whereas the WD-BC/CNT fibers (treated with PSE only) do not fluoresce, indicating the introduction of PSE, which is also confirmed by infrared spectroscopy (Fig. 2b and Fig. S6, S7). Furthermore, the distribution of C, N, and Si across the cross-section of muscle-inspired fibers revealed by energy dispersive X-ray

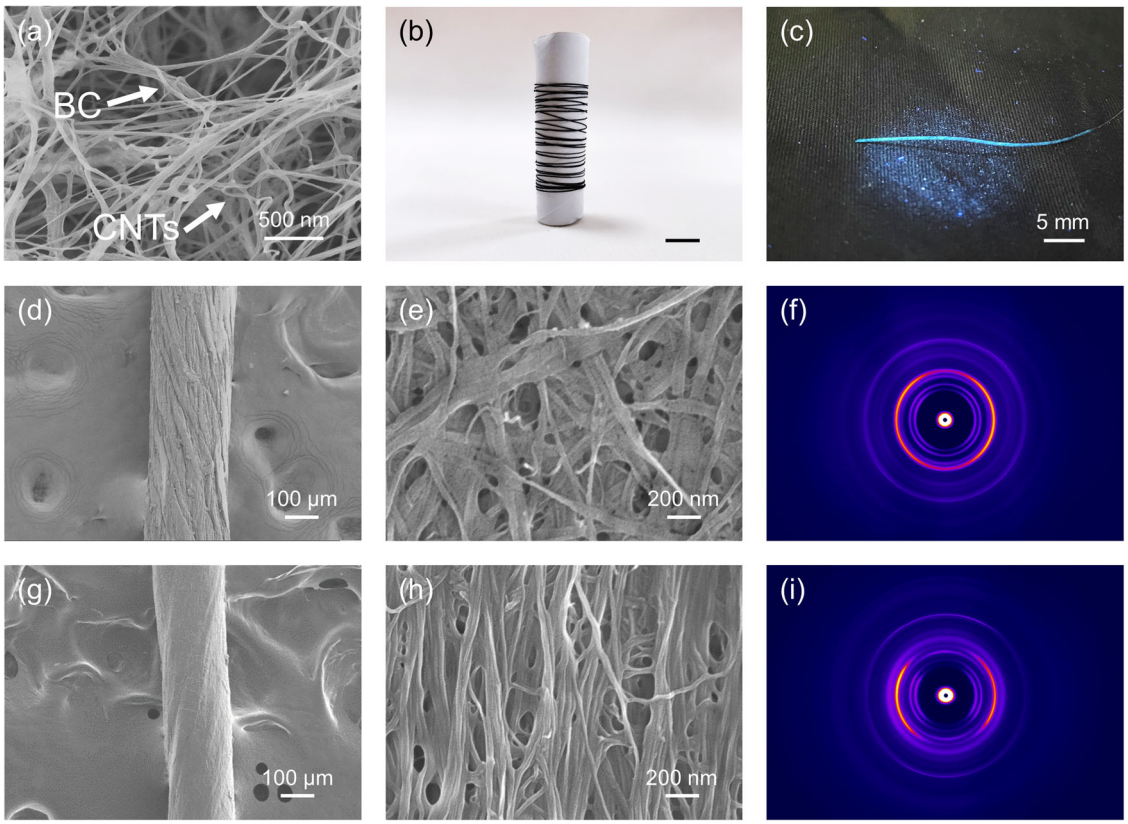

Fig. 2 Characterization of the composite fibers (15.9 wt% CNT). a Scanning electron microscopy (SEM) image of the composite hydrogel, showing the uniform distribution of CNTs in the BC network. **b** A roll of the muscle-inspired fiber. The scale bar corresponds to 1 cm. **c** The fluorescence of muscle-inspired fibers is excited under ultraviolet light. **d** SEM image of the composite fibers with only wet twisting (BC/CNT fibers), showing a rough surface. **e** SEM image of the BC/CNT fibers, showing randomly oriented CNTs and BC nanofibers. **f** Two-dimensional wide-angle X-ray diffraction (2D-WAXD) patterns of BC/CNT fibers. **g** SEM image of the composite fibers with wet drawing and wet twisting (WD-BC/CNT fibers), showing a smooth surface. **h** SEM image of WD-BC/CNT fibers, showing a highly aligned structure. **i** The 2D-WAXD pattern of WD-BC/CNT fibers.

spectrometry directly confirms the uniformity of the reaction within the fiber (Fig. S8).

Mechanical properties of the muscle-inspired fibers

Benefiting from the 3D network of BC and the enhancements to structure and interaction brought by physical and chemical treatment, respectively, the muscle-inspired fibers exhibit better mechanical properties than most natural fibers, indicating the superiority of the muscle-inspired structure (Figs. 1h, 3c and Table S1). With a diameter of approximately 0.21 mm, the muscle-inspired fiber can stably be loaded with a weight of 0.5 kg for 2 h, which allows it to be used for the suspension of light bulbs (Fig. 1i, j).

To investigate the influence of wet drawing and chemical treatment, the stress–strain curves of the composite fibers were systematically measured. As shown in Fig. 3a, b, the tensile strength and Young's modulus of BC/CNT fibers can only reach ~201 MPa and ~4.8 GPa, respectively, which is due to the loose network structure inside the composite fibers and the poor interaction between components (Fig. 3d, g). After oriented wet drawing, the tensile strength of the composite fibers is greatly improved to ~736 MPa, while the strain to failure dramatically decreases from 5.8% to 2.7%, leading to an approximately 7-fold increase in Young's modulus to 38 GPa (Fig. 3b). The SEM images of fracture surfaces reveal a dense oriented structure after oriented wet drawing, which contributes to the formation of a dense hydrogen bonding network between aligned BC nanofibers, prompting an increase in strength and stiffness (Fig. 3e, h). Based on the dense oriented structure, the introduction of PSE to cellulose can further increase the strength and stiffness to 939 MPa and 52.3 GPa, respectively, which is attributed to the tight combination between cellulose-PSE and CNTs through π-π interactions (Fig. 3f, i). In contrast, after the chemical treatment process, the strength and Young's modulus of pure BC fibers were almost unchanged, which indicates that the chemical treatment does not enhance interactions within BC fibers (Fig. S9, S10).

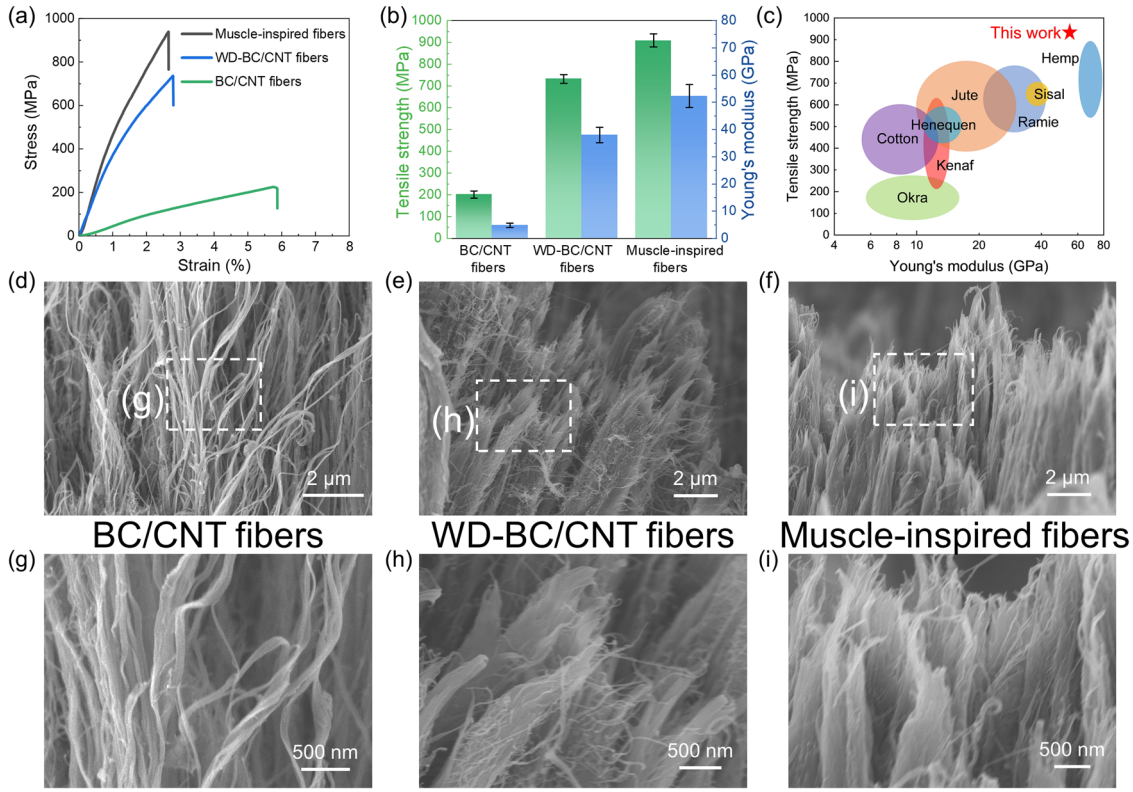

Fig. 3 Mechanical properties of the muscle-inspired fibers (15.9 wt% CNT). a Tensile stress–strain curves of the muscle-inspired fibers, WD-BC/CNT fibers, and BC/CNT fibers. **b** Comparison of the tensile strength and stiffness of the muscle-inspired fibers, WD-BC/CNT fibers, and BC/CNT fibers. **c** Ashby diagram of tensile strength vs. stiffness for the muscle-inspired fiber compared with natural plant fibers. **d**, **g** SEM images of BC/CNT fibers, showing a loose network structure. **g** shows the enlarged view of the area framed in **d**. **e**, **h** SEM images of WD-BC/CNT fibers, showing a dense oriented structure. **h** shows the enlarged view of the area framed in **e**. **f**, **i** SEM images of the muscle-inspired fibers, showing a tight combination of BC and CNTs. **i** shows the enlarged view of the area framed in **f**.

In addition, we measured the mechanical performance of pure BC fibers and muscle-inspired composite fibers with different contents of CNTs, showing that the strength first increases and then decreases with increasing CNT content (Figs. S10, S11), reflecting the trade-off between the CNT content and the degree of wet drawing. With a fiber of low CNT content, the stress within the fiber can be better dispersed through the interaction between the components by increasing the CNT content, which contributes to the improvement in strength. At a high CNT content, the final wet-drawing degree decreases and then affects the mechanical strength of the fibers, which can be attributed to the weakened ability of the hydrogel to withstand wet drawing with a reduction in the BC content.

Based on the enhancement brought by wet drawing and chemical treatment, the muscle-inspired fibers are endowed with superior mechanical properties compared to other natural fibers (Figs. 1h, 3c and Table S1)[32–37]. Not only does the strength of the muscle-inspired fibers surpass that of hemp fibers, one of the strongest natural plant fibers but also the Young's modulus exceeds that of sisal fibers, one of the hardest natural plant fibers. Compared with other conductive fibers reported in the literature[11,12,14,15,39,40], which mainly focuses on the improvement of electrical conductivity and strain to failure, the muscle-inspired fibers possess considerable advantages in strength (Table S2), giving them great potential for application in high-performance conductive fiber-based composites.

In addition to high mechanical strength and stiffness, muscle-inspired fibers exhibit excellent fatigue resistance, which is important to maintain stable mechanical properties during long-term use. To further explore the applicability of our muscle-inspired fibers in practical surroundings, bending tests were systematically carried out in which samples were clamped with a bob-weight of 50 g (Fig. S12). After 100,000 cycles of the bending test with an angle of 120°, the bending behavior of muscle-inspired fibers remained almost unchanged, similar to that of pure BC fibers (Fig. 4a and Fig. S13), demonstrating the high stability of the continuous 3D network of BC. As shown in Fig. 4b, compared with the morphologies before the bending test, the surface of muscle-inspired fibers after

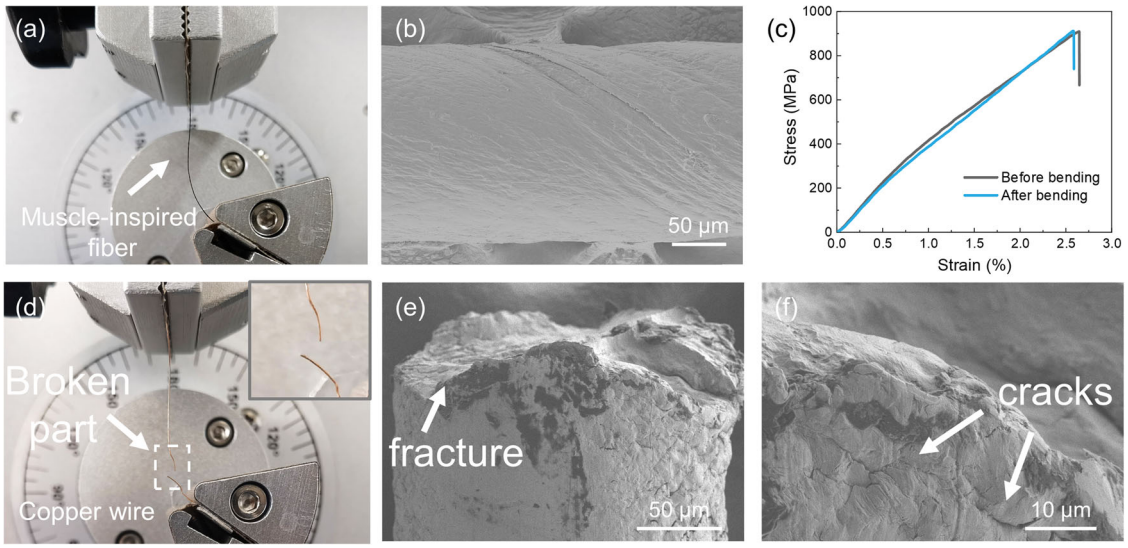

Fig. 4 The fatigue resistance of the muscle-inspired fibers (15.9 wt% CNT). a Muscle-inspired fibers in the bending test. **b** SEM image of the muscle-inspired fibers with a diameter of ~190 μm after the bending test. **c** Tensile stress–strain curves of the muscle-inspired fibers before and after 100,000 cycles of the bending test. **d** A common conductive copper wire breaks after 400 cycles of the bending test. The inset photograph is an enlarged view of the broken part. **e** SEM image of the broken part of the copper wire with a diameter of ~200 μm, showing a relatively smooth fracture surface. **f** SEM image of the area around the fracture, showing the cracks from repeated bending.

the bending test remains mostly glossy, with only a few small cracks (Figs. S14, S15). Based on the 3D network structure of BC, the muscle-inspired fibers feature excellent mechanical stability, which is further confirmed by the almost unchanged stress–strain curves (99.6% tensile strength retention) before and after the bending test (Fig. 4c). In contrast, after approximately 400 cycles of bending, common conductive copper wires always break and show multiple cracks expanding along the radial direction and a smooth fatigue fracture surface in the broken part (Fig. 4d–f and Fig. S16). The high fatigue resistance of muscle-inspired fibers, which far exceeds that of common metal-based conductive fibers, is expected to result in the construction of high-performance materials for complex use.

Muscle-inspired fibers for sensing and self-monitoring

Benefiting from the muscle-inspired design, the composite fibers also have improved electrical properties. To systematically study the electrical properties of the muscle-inspired fibers, their electrical conductivity was measured in detail. As shown in Fig. 5a, all the muscle-inspired fibers with different CNT contents exhibit typical I–V curves at room temperature, indicating a feature similar to pure resistance. As the CNT content increased from 15.9% to 42.4%, the electrical conductivity of muscle-inspired fibers significantly increased from 516 S m^{-1} to 1719 S m^{-1} (Fig. 5b) due to the formation of more conductive pathways. These muscle-inspired fibers possess high electrical conductivity similar to that of WD-BC/CNT fibers and show a slight advantage over BC/CNT composite fibers, which is attributed to the oriented muscle-inspired design that can effectively reduce the connection nodes between CNTs within the same length[41]. Furthermore, the excellent mechanical stability given by the robust structure promises the stability of electrical performance. Even after 100,000 cycles of the bending test, the electrical conductivity of the conductive fiber remains almost unchanged, making it an ideal candidate for constructing conductive functional devices for long-term use (Fig. 5c).

With the combination of excellent mechanical and electrical properties, muscle-inspired fibers possess great potential as carriers for signal transmission to be integrated into functional devices, including functions related to sensing and monitoring. Based on the design shown in Fig. 5d and Fig. S17, the muscle-inspired fibers were successfully integrated into ordinary fingerstalls, enabling them to effectively sense the bending of fingers[42]. When the finger bends, the length change of the elastic cord causes the muscle-inspired fiber to slide past the wire contact point in the middle of the fingerstall, which makes the conductive fiber between the two wire contact points longer and results in an increase in electrical resistance. Through the simultaneous monitoring and analysis of the movement of five fingers, various gestures can be effectively distinguished, providing guidance for overall behavior prediction (Fig. 5e).

Furthermore, similar to other high-performance fibers, muscle-inspired fibers are also suitable for preparing fiber-based composite materials with resin or ceramics, giving them the added advantage of self-monitoring

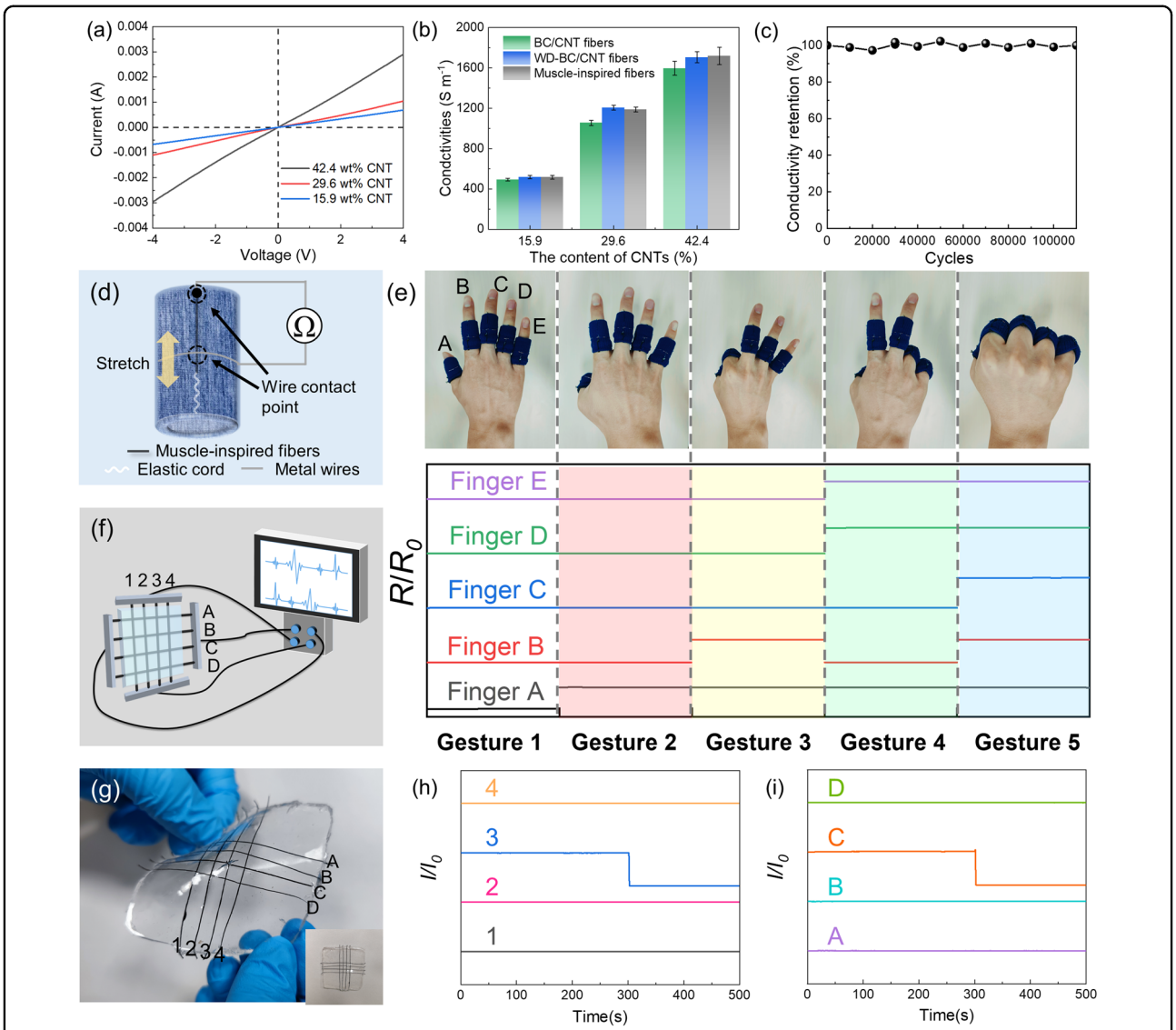

Fig. 5 The electrical properties and sensing performance of the muscle-inspired fibers. a Typical I–V curves of muscle-inspired fibers with different CNT contents showing their pure resistance. **b** The electrical conductivity of the muscle-inspired fibers, WD-BC/CNT fibers and BC/CNT fibers with different CNT contents. **c** The electrical conductivities of the muscle-inspired fibers after different numbers of bending test cycles. **d** Schematic illustration of the fiber-based smart fingerstalls. **e** Photograph of the muscle-inspired fiber-based smart fingerstalls worn on the hand. The upper wire contact point is fixed, and the middle wire contact point is slidable. Different letters correspond to the fingerstalls on different fingers. With the change in gestures, the muscle-inspired fiber-based smart fingerstalls provide different signals through the current. The signals reflect the resistance changes of the muscle-inspired fibers between the two wire contact points. **f** Schematic illustration of the conductive fiber-based composite with a sensing function. **g** The muscle-inspired fiber-based composite after damage. The inset photograph is the muscle-inspired fiber-based composite before damage. **h, i** The self-monitoring of the muscle-inspired fiber-based composite through electric current. The signals reflect the current changes of muscle-inspired fibers.

function through current. To confirm the validity of the self-monitoring function, muscle-inspired fibers, which overlap each other vertically to form the network structure, were used to reinforce polydimethylsiloxane for systematic study (Fig. 5f, g). Benefiting from the electrical conductivity of the muscle-inspired fibers, damaged fibers inside the composite material exhibit a drastic change in the current signal during the injury process. Through this process, the damage location can be accurately identified, which matches the location of the damage seen, demonstrating an excellent ability to warn of injury (Fig. 5h, i). This means that even if the composite materials with the muscle-inspired fibers are in a location invisible to the naked eye, their condition can still be monitored in real time by the current, which contributes to not only prolonging the service life of the material but also achieving early warning of injury to avoid causing greater harm.

Conclusions

In summary, inspired by the exquisite fascicle structure of skeletal muscle, a method of in situ biosynthesis and physical and chemical enhancement has been proposed to fabricate high-performance conductive fibers. With the aerosol-assisted biosynthesis strategy for composite preparation, a robust uniform composite hydrogel is obtained with CNTs entangled in situ in a 3D network of BC. After wet drawing and wet twisting to attain the dense oriented structure and the chemical treatment for component bridging, uniformly distributed CNTs form a tight bond with the oriented 3D network of BC. Benefitting from the bioinspired design, the composite fibers achieve the integration of outstanding mechanical properties, including high strength (939 MPa), high stiffness (52.3 GPa), high fatigue resistance (a high tensile strength retention of 99.6% after 100,000 bending cycles), and stable electrical performance. Based on these excellent properties, muscle-inspired fibers have the potential to play a key role in future intelligent fiber-based composites and smart flexible devices.

Materials and methods

Preparation of the muscle-inspired fibers

All reagents were commercially available. The CNTs (category No: TNMC2) purchased from Chengdu Zhongke Times Nano Energy Tech Co., Ltd. feature an outer diameter of 8–15 nm and a length of ~50 μm; dimensions are provided by the manufacturer. First, *Gluconacetobacter xylinus* 1.1812 (China General Microbiological Culture Collection Center, CGMCC), a bacterial strain, was inoculated onto a solid agar substrate at 28 °C. After 24 h, a thin pure BC film was formed. Then, through the intermittent spray of CNT suspension (0.5 wt%) with filtered compressed air, continuous liquid nutrient/CNT aerosol was produced and fed on the BC film. After 5 d of aerosol-assisted biosynthesis, a uniform BC/CNT hydrogel was prepared[26–28]. Next, the BC/CNT hydrogels were washed and cut into strips and then repeatedly wet drawn and shaken until they could no longer be stretched. The wet-drawing degrees of pure BC fiber, 15.9 wt% CNT fiber, 29.6 wt% CNT fiber and 42.4 wt% CNT fiber were ~32%, ~24%, ~13%, and ~4%, respectively. The degree of wet drawing is defined as the percentage of the increased length of the hydrogel strips after wet drawing to the original length. BC/CNT strips were then immediately transformed into dense fibers through the repeated alternating wet twisting and shaft smoothing process operated by two hands. The wet-twisting degrees of all these fibers were ~5.2 turns per centimeter. After that, the dense fibers were immersed in an *N,N*-dimethylformamide solution (40 mL) of (3-aminopropyl)triethoxysilane (APTES) (0.85 mol L^{-1}) for 1 d, removed, heated at 105 °C for 30 min, and then washed more than three times. Finally, the dense fibers were immersed in an *N,N*-dimethylformamide solution of 1-pyrenebutyric acid N-hydroxysuccinimide ester (PSE) (24 mmol L^{-1}) for 1 d, followed by washing more than three times and drying[29].

Note

The experiments involving human subjects have been performed by the authors of the manuscript. The research process was harmless to humans, and their consent was obtained.

Acknowledgements

This work was supported by the National Natural Science Foundation of China (Grants 51732011, U1932213, 22105194, 92163130), the National Key Research and Development Program of China (Grants 2021YFA0715700 and 2018YFE0202201), the University Synergy Innovation Program of Anhui Province (Grant GXXT-2019-028), and Anhui Provincial Key R&D Programs (202104a05020013).

Funding

The National Natural Science Foundation of China (Grant Nos. 51732011, U1932213, 22105194, and 92163130), the National Key Research and Development Program of China (Grant Nos. 2021YFA0715700 and 2018YFE0202201), the University Synergy Innovation Program of Anhui Province (Grant No. GXXT-2019-028), and Anhui Provincial Key R&D Programs (202104a05020013).

Author contributions

Q.-F.G., and S.-H.Y. conceived the idea and designed the experiments. S.-H.Y. supervised the project. Q.-F.G., Z.-C.L., and H.-B.Y. carried out the synthetic experiment and analysis. Z.Z. and K.-P.Y. contributed to the 3D illustrations. Z.-C.L., Q.-F.G., and S.-H.Y. wrote the paper, and all authors discussed the results and commented on the manuscript.

Conflict of interest

The authors declare that they have no conflict of interest.

Supplementary information The online version contains supplementary material available at https://doi.org/10.1038/s41427-023-00461-4.

Received: 18 August 2022 Revised: 7 December 2022 Accepted: 12 December 2022.
Published online: 31 March 2023

References

1. He, J. et al. Scalable production of high-performing woven lithium-ion fibre batteries. *Nature* **597**, 57–63 (2021).
2. Lu, C. et al. Flexible and stretchable nanowire-coated fibers for optoelectronic probing of spinal cord circuits. *Sci. Adv.* **3**, e1600955 (2017).
3. Shi, X. et al. Large-area display textiles integrated with functional systems. *Nature* **591**, 240–245 (2021).
4. Xiong, J., Chen, J. & Lee, P. S. Functional fibers and fabrics for soft robotics, wearables, and human-robot interface. *Adv. Mater.* **33**, 2002640 (2021).
5. Guan, Q.-F. et al. Bio-inspired lotus-fiber-like spiral hydrogel bacterial cellulose fibers. *Nano Lett.* **21**, 952–958 (2021).
6. Dong, K., Peng, X. & Wang, Z. L. Fiber/fabric-based piezoelectric and triboelectric nanogenerators for flexible/stretchable and wearable electronics and artificial intelligence. *Adv. Mater.* **32**, 1902549 (2020).

7. Lee, J. et al. Conductive fiber-based ultrasensitive textile pressure sensor for wearable electronics. *Adv. Mater.* **27**, 2433–2439 (2015).
8. Zhang, X., Lu, W., Zhou, G. & Li, Q. Understanding the mechanical and conductive properties of carbon nanotube fibers for smart electronics. *Adv. Mater.* **32**, 1902028 (2020).
9. Hu, S. et al. Biodegradable, super-strong, and conductive cellulose macrofibers for fabric-based triboelectric nanogenerator. *Nano-Micro Lett.* **14**, 115–115 (2022).
10. Chen, X. Making electrodes stretchable. *Small Methods* **1**, 1600029 (2017).
11. Gao, J. et al. Ultra-robust and extensible fibrous mechanical sensors for wearable smart healthcare. *Adv. Mater.* **34**, 2107511 (2022).
12. Lee, S. et al. Ag nanowire reinforced highly stretchable conductive fibers for wearable electronics. *Adv. Funct. Mater.* **25**, 3114–3121 (2015).
13. Kwon, C. et al. Self-bondable and stretchable conductive composite fibers with spatially controlled percolated Ag nanoparticle networks: novel integration strategy for wearable electronics. *Adv. Funct. Mater.* **30**, 2005447 (2020).
14. Cooper, C. B. et al. Toughening stretchable fibers via serial fracturing of a metallic core. *Sci. Adv.* **5**, eaat4600 (2019).
15. Wang, H. et al. Downsized sheath-core conducting fibers for weavable superelastic wires, biosensors, supercapacitors, and strain sensors. *Adv. Mater.* **28**, 4998–5007 (2016).
16. Kausar, A., Rafique, I. & Muhammad, B. Aerospace application of polymer nanocomposite with carbon nanotube, graphite, graphene oxide, and nanoclay. *Polym.-Plast. Technol. Eng.* **56**, 1438–1456 (2017).
17. Deka, B. K., Hazarika, A., Kim, J., Park, Y. B. & Park, H. W. Recent development and challenges of multifunctional structural supercapacitors for automotive industries. *Int. J. Energy Res.* **41**, 1397–1411 (2017).
18. Wegst, U. G., Bai, H., Saiz, E., Tomsia, A. P. & Ritchie, R. O. Bioinspired structural materials. *Nat. Mater.* **14**, 23–36 (2015).
19. Meyers, M. A., McKittrick, J. & Chen, P.-Y. Structural biological materials: critical mechanics-materials connections. *Science* **339**, 773–779 (2013).
20. Barthelat, F., Yin, Z. & Buehler, M. J. Structure and mechanics of interfaces in biological materials. *Nat. Rev. Mater.* **1**, 16007 (2016).
21. Gillies, A. R. & Lieber, R. L. Structure and function of the skeletal muscle extracellular matrix. *Muscle Nerve* **44**, 318–331 (2011).
22. Turrina, A., Martinez-Gonzalez, M. A. & Stecco, C. The muscular force transmission system: role of the intramuscular connective tissue. *J. Bodyw. Mov. Ther.* **17**, 95–102 (2013).
23. Purslow, P. P. The Structure and role of intramuscular connective tissue in muscle function. *Front. Physiol.* **11**, 495 (2020).
24. Sharafi, B. & Blemker, S. S. A mathematical model of force transmission from intrafascicularly terminating muscle fibers. *J. Biomech.* **44**, 2031–2039 (2011).
25. Zhang, W., Liu, Y. & Zhang, H. Extracellular matrix: an important regulator of cell functions and skeletal muscle development. *Cell Biosci* **11**, 65 (2021).
26. Guan, Q.-F. et al. A general aerosol-assisted biosynthesis of functional bulk nanocomposites. *Natl. Sci. Rev.* **6**, 64–73 (2019).
27. Guan, Q.-F. et al. Sustainable 3D structural binder for high-performance supercapacitor by biosynthesis process. *Adv. Funct. Mater.* **31**, 2105070 (2021).
28. Guan, Q.-F., Ling, Z.-C., Han, Z.-M., Yang, H.-B. & Yu, S.-H. Ultra-strong, ultra-tough, transparent, and sustainable nanocomposite films for plastic substitute. *Matter* **3**, 1308–1317 (2020).
29. Wan, S. et al. Sequentially bridged graphene sheets with high strength, toughness, and electrical conductivity. *Proc. Natl Acad. Sci. USA* **115**, 5359–5364 (2018).
30. Yang, Q. & Pan, X. A facile approach for fabricating fluorescent cellulose. *J. Appl. Polym. Sci.* **117**, 3639–3644 (2010).
31. Neves, R. M., Ornaghi, H. L. Jr., Zattera, A. J. & Amico, S. C. The influence of silane surface modification on microcrystalline cellulose characteristics. *Carbohydr. Polym.* **230**, 115595 (2020).
32. Sathishkumar, T. P., Navaneethakrishnan, P., Shankar, S., Rajasekar, R. & Rajini, N. Characterization of natural fiber and composites: a review. *J. Reinf. Plast. Comp.* **32**, 1457–1476 (2013).
33. Li, X., Tabil, L. G. & Panigrahi, S. Chemical treatments of natural fiber for use in natural fiber-reinforced composites: a review. *J. Polym. Environ.* **15**, 25–33 (2007).
34. Bledzki, A. K. & Gassan, J. Composites reinforced with cellulose based fibres. *Prog. Polym. Sci.* **24**, 221–274 (1999).
35. Nam, S. & Netravali, A. N. Green composites. I. Physical properties of ramie fibers for environment-friendly green composites. *Fibers Polym* **7**, 372–379 (2006).
36. Fuqua, M. A., Huo, S. & Ulven, C. A. Natural fiber reinforced composites. *Polym. Rev.* **52**, 259–320 (2012).
37. Mohammed, L., Ansari, M. N. M., Pua, G., Jawaid, M. & Islam, M. S. A review on natural fiber reinforced polymer composite and its applications. *Int. J. Polym. Sci.* **2015**, 243947 (2015).
38. Wang, S. et al. Super-strong, super-stiff macrofibers with aligned, long bacterial cellulose nanofibers. *Adv. Mater.* **29**, 1702498 (2017).
39. Jiang, S. et al. Highly stretchable conductive fibers from few-walled carbon nanotubes coated on poly(m-phenylene isophthalamide) polymer core/shell structures. *ACS Nano* **9**, 10252–10257 (2015).
40. Zhou, G. et al. High-strength single-walled carbon nanotube/permalloy nanoparticle/poly(vinyl alcohol) multifunctional nanocomposite fiber. *ACS Nano* **9**, 11414–11421 (2015).
41. Du, F. M., Fischer, J. E. & Winey, K. I. Effect of nanotube alignment on percolation conductivity in carbon nanotube/polymer composites. *Phys. Rev. B* **72**, 121404 (2005).
42. Gibbs, P. T. & Asada, H. H. Wearable conductive fiber sensors for multi-axis human joint angle measurements. *J. NeuroEngineering Rehabil.* **2**, 7 (2005).